Science Advances
AAAS

Supplementary Materials for

A probiotic nanozyme hydrogel regulates vaginal microenvironment for *Candida* vaginitis therapy

Gen Wei *et al.*

Corresponding author: Hui Wei, weihui@nju.edu.cn

Sci. Adv. **9**, eadg0949 (2023)
DOI: 10.1126/sciadv.adg0949

This PDF file includes:

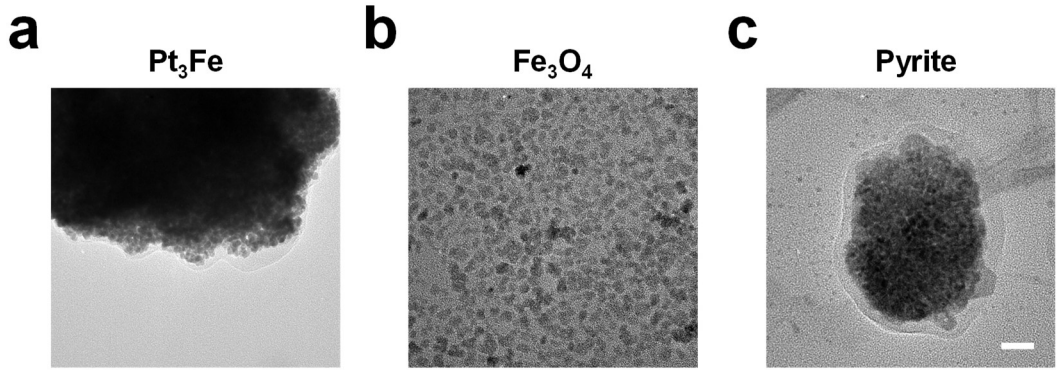

Fig. S1. TEM images of Pt_3Fe (a), Fe_3O_4 (b), and Pyrite FeS_2 (c) nanozymes. Scale bar: 20 nm.

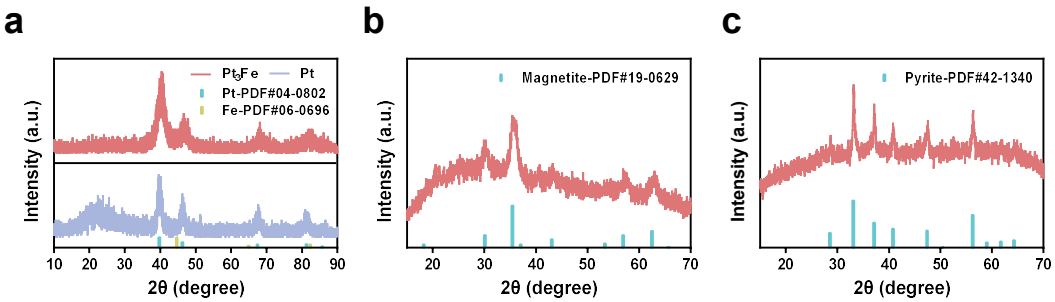

Fig. S2. XRD patterns of Pt_3Fe (a), Fe_3O_4 (b), and Pyrite FeS_2 (c) nanozymes. The lines at the bottom mark the reference patterns of Pt (JCPDS card number 04-0802), Fe (JCPDS card number 06-0696), Magnetite Fe_3O_4 (JCPDS card number 19-0629), and Pyrite FeS_2 (JCPDS card number 42-1340).

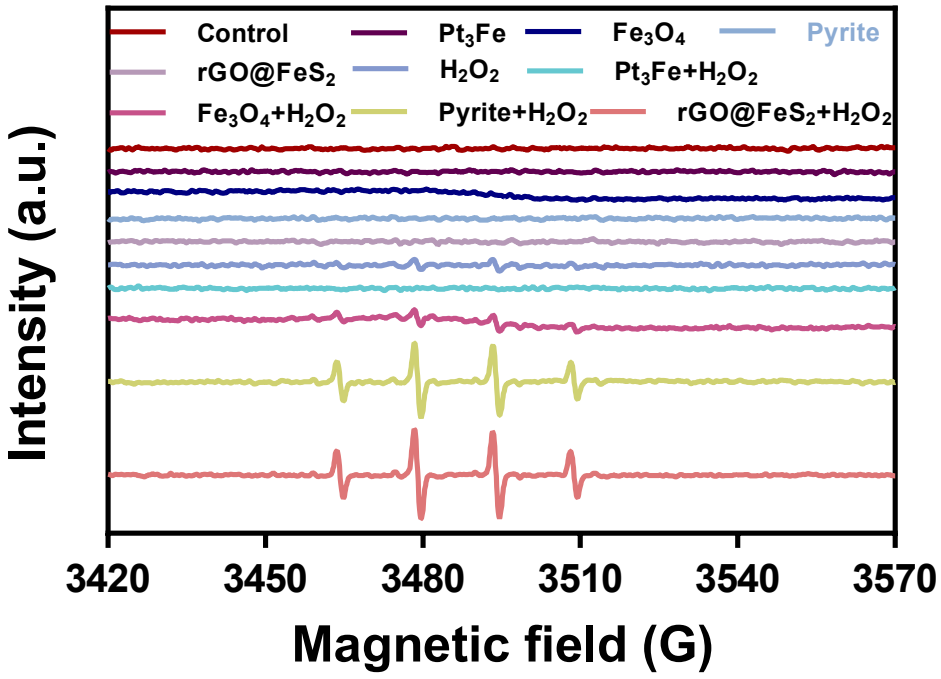

Fig. S3. EPR spectra monitoring the formation of ˙OH among Pt_3Fe, Fe_3O_4, Pyrite FeS_2, and rGO@FeS_2 nanozymes with H_2O_2 (80 μM).

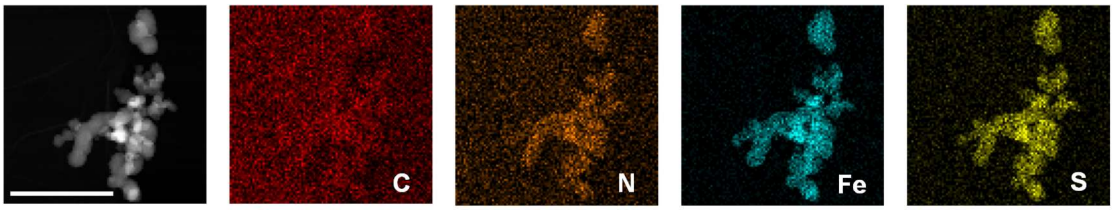

Fig. S4. Element mapping of rGO@FeS_2 nanozymes. Scale bar: 500 nm.

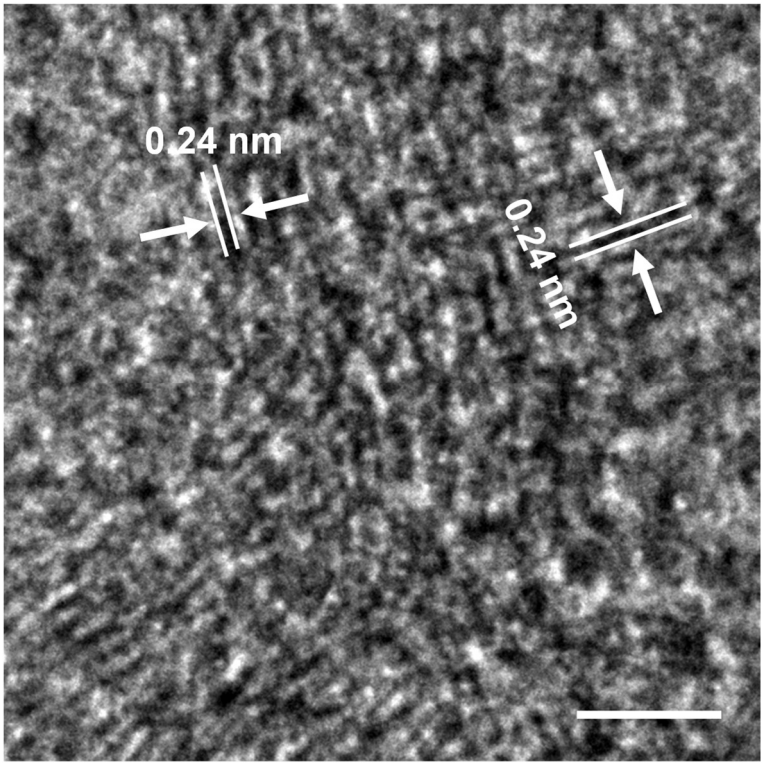

Fig. S5. HRTEM image of rGO@FeS_2 nanozymes. Scale bar: 5 nm.

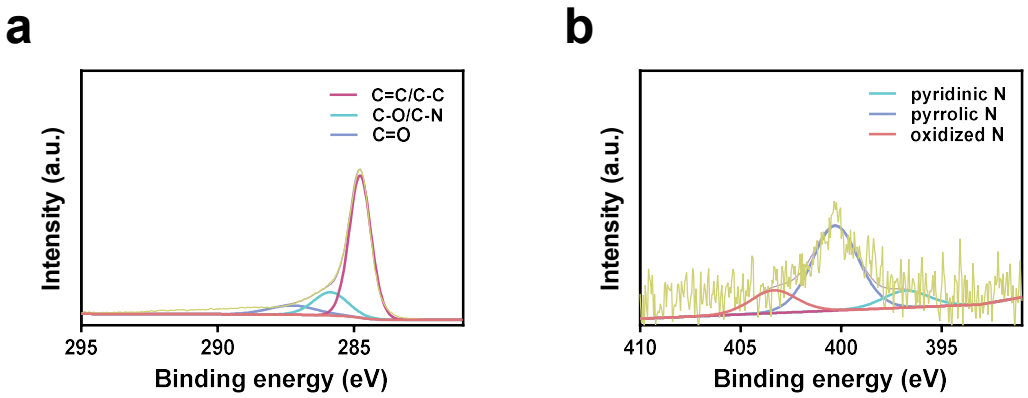

Fig. S6. XPS spectra for C 1*s* (a) and N 1*s* (b) regions of rGO@FeS_2 nanozymes.

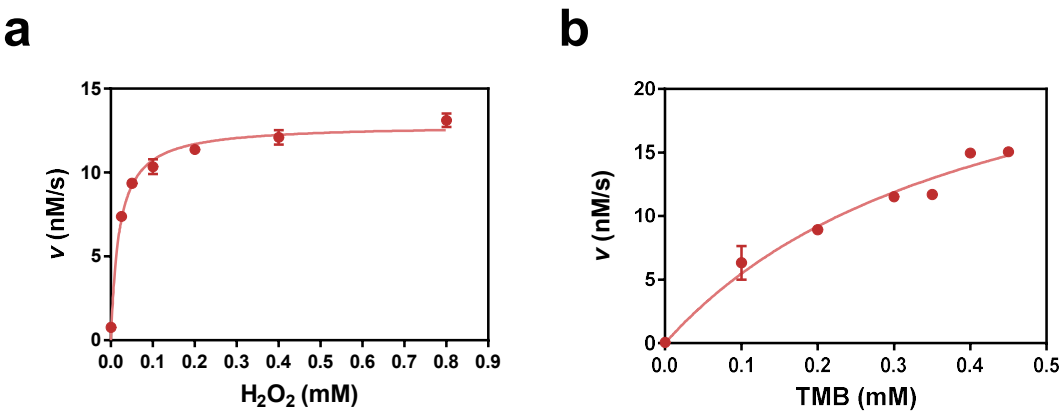

Fig. S7. Michaelis–Menten plots with varying concentrations of H_2O_2 (a) and TMB (b) as substrates for the POD-like activity of rGO@FeS_2 nanozymes.

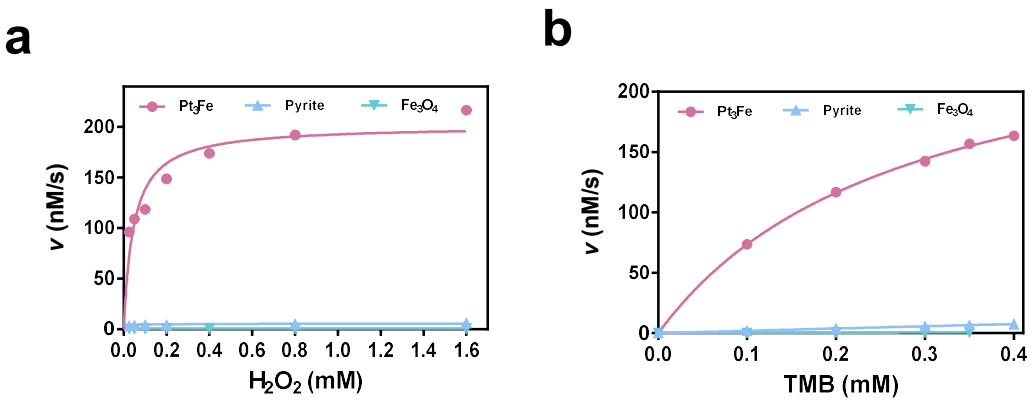

Fig. S8. Michaelis–Menten plots with varying concentrations of H_2O_2 (a) and TMB (b) as substrates for the POD-like activity of several other nanozymes (Pt_3Fe, Pyrite, and Fe_3O_4 nanozymes). The concentration of Pt_3Fe nanozymes was diluted 20-fold under the same iron content.

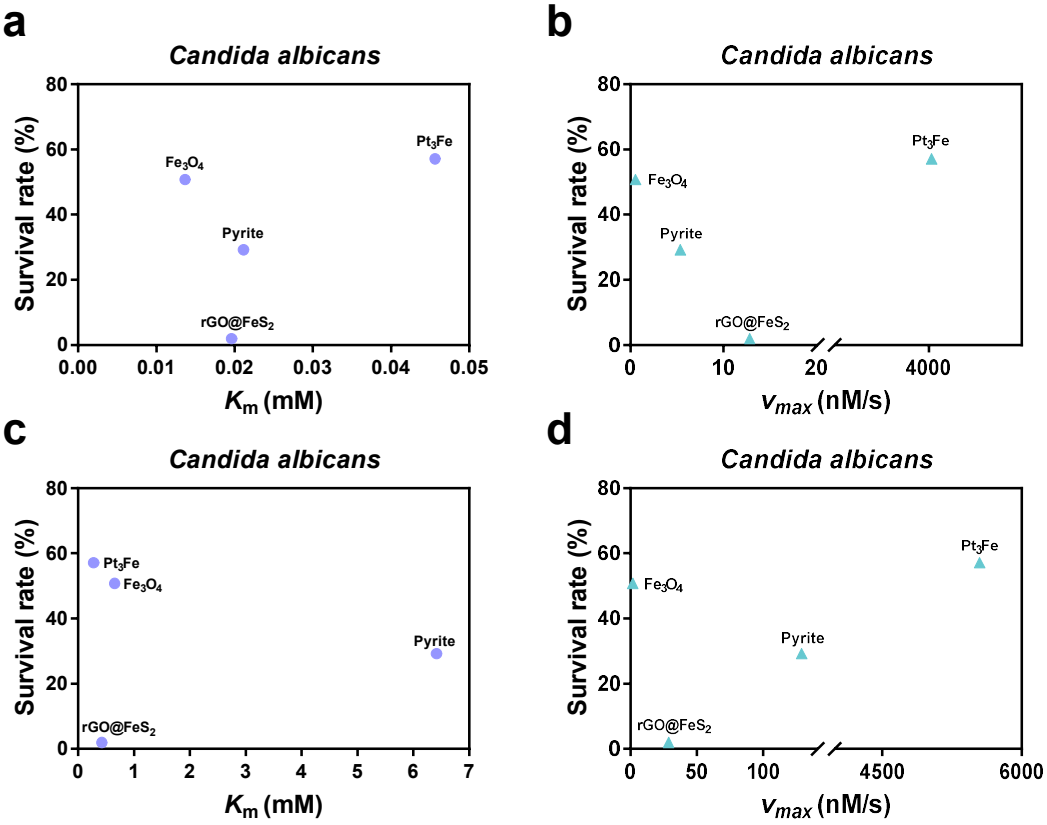

Fig. S9. Plots showing the relationship between *anti-Candida albicans* activity and the kinetics data of four POD-like nanozymes with H_2O_2 (a, b) or TMB (c, d) as substrate.

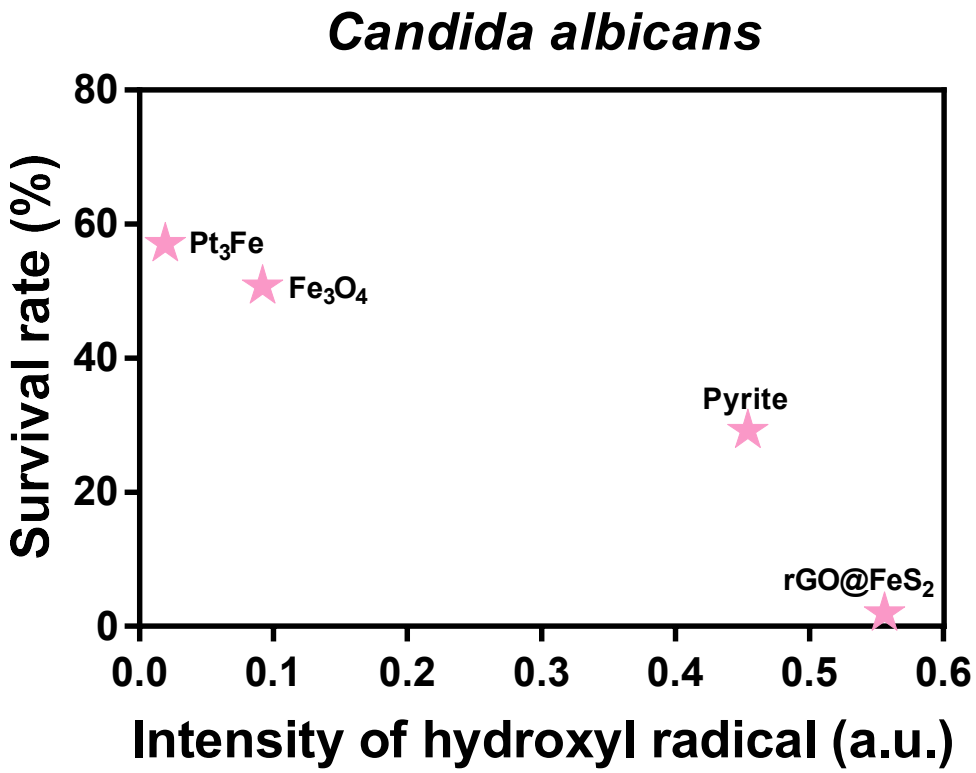

Fig. S10. A plot showing the relationship between the formation of ˙OH and anti-*Candida albicans* activities among Pt_3Fe, Fe_3O_4, Pyrite FeS_2, and rGO@FeS_2 nanozymes with H_2O_2 (80 μM).

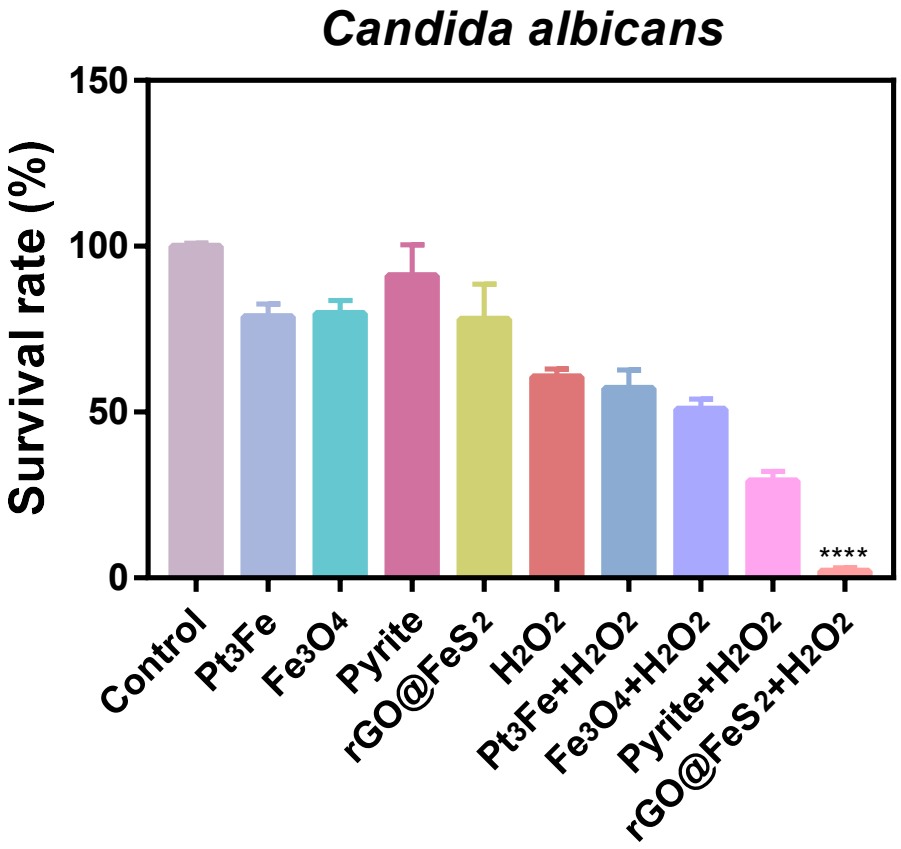

Fig. S11. Comparison of anti-*Candida albicans* activities of different nanozymes after indicated treatments. Data are presented as mean ± SD (n = 3).

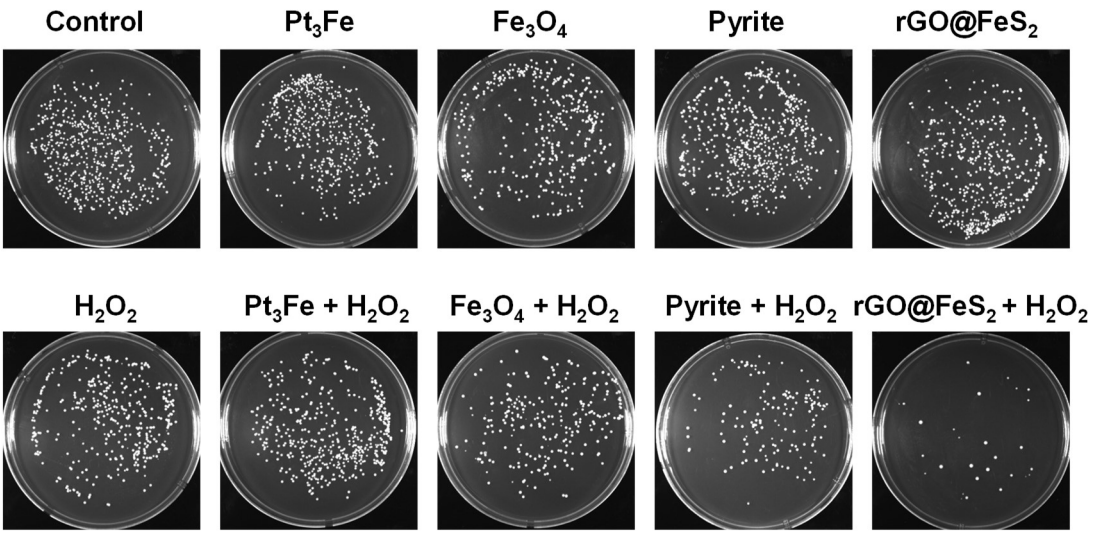

Fig. S12. Digital images of *Candida albicans* colonies after indicated treatments.

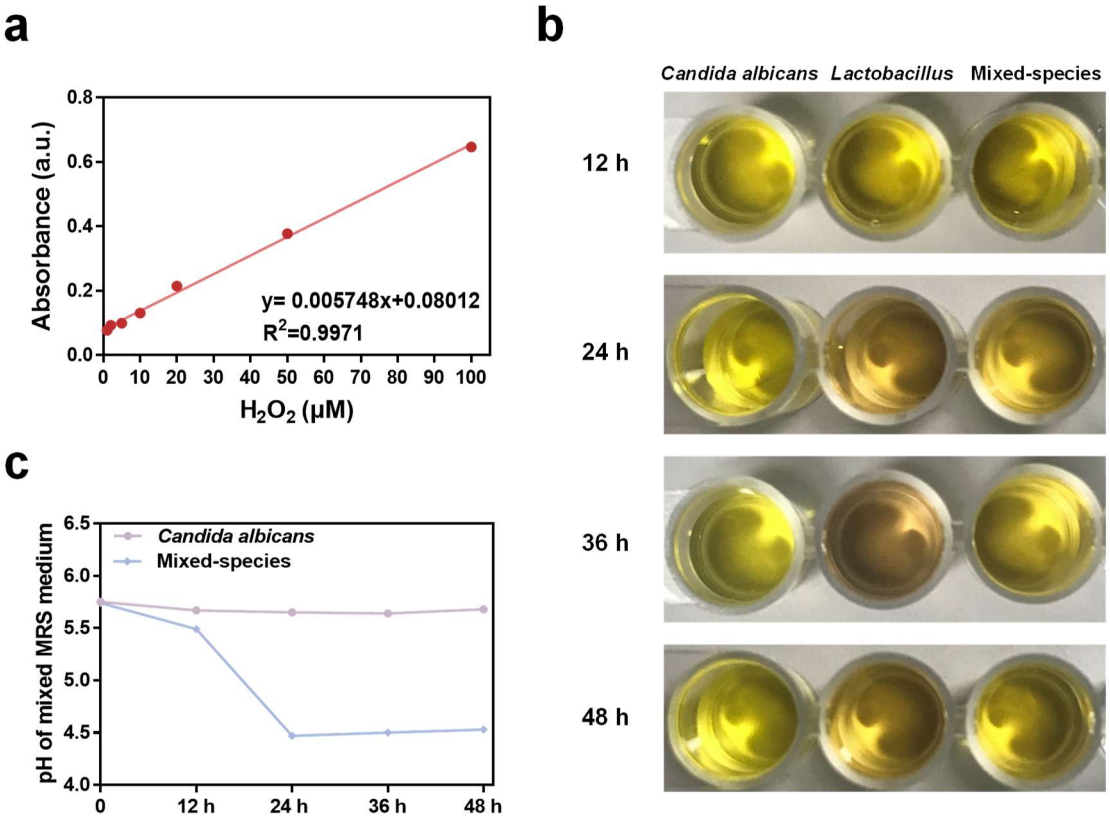

Fig. S13. Determination of H_2O_2 and pH change of MRS medium after different incubation times. The amounts of H_2O_2 were detected via the following principle: H_2O_2 first reacts with Fe^{2+} to produce Fe^{3+}; then, the Fe^{3+} reacts with xylenol orange to form a purple product. **a, b**, H_2O_2 standard curve (**a**) and color changes of substrate after reacting with H_2O_2 for different times in MRS medium containing *Candida albicans*, *Lactobacillus* and mixed-species (**b**). **c**, pH changes of MRS medium in *Candida albicans* and mixed-species groups after different incubation times. The culture conditions were microaerophilic.

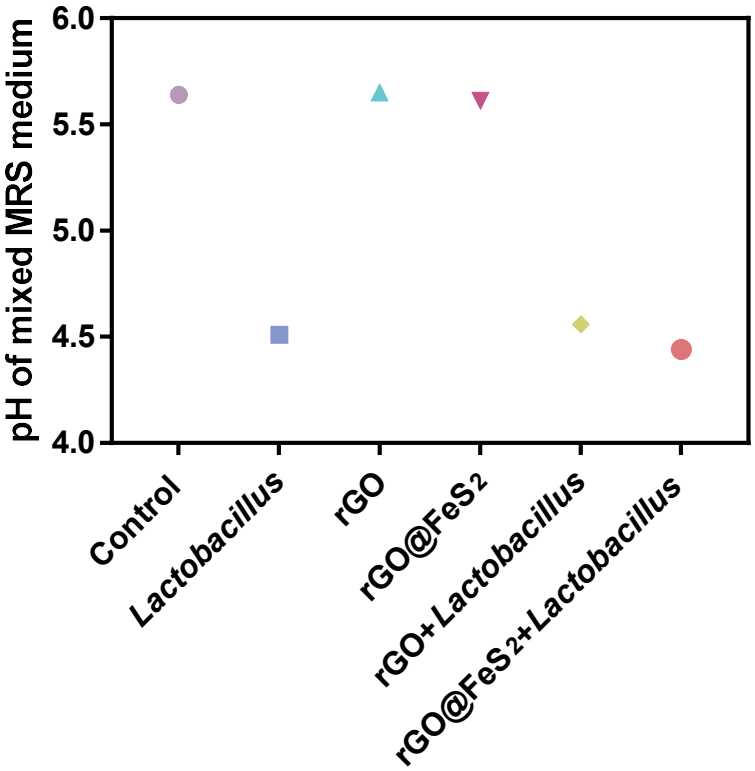

Fig. S14. pH of MRS medium in the indicated groups.

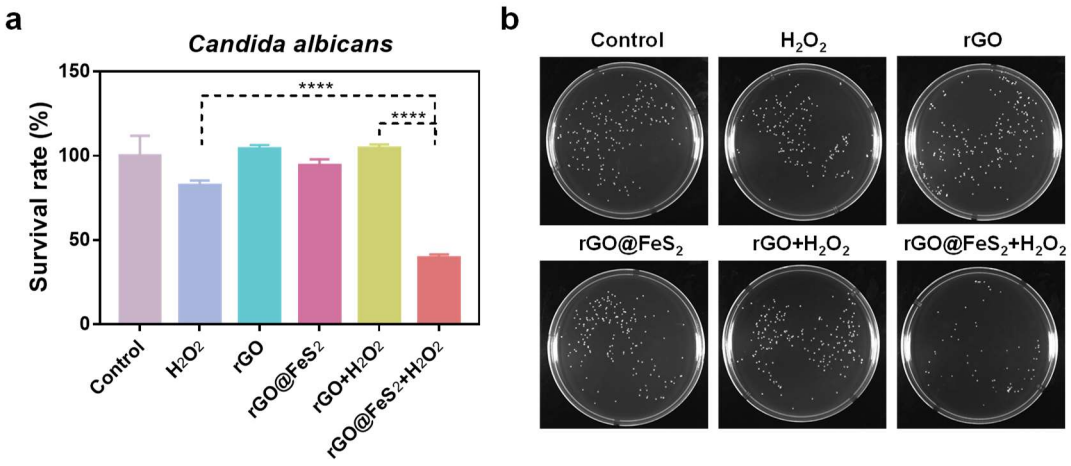

Fig. S15. Anti-*Candida albicans* activity of rGO@FeS_2 with a lower concentration of H_2O_2. Antifungal effects (**a**) and digital images of *Candida albicans* colonies (**b**) after indicated treatments. A 30 μM amount of H_2O_2, rGO and rGO@FeS_2 at 25 μg/mL was used for anti-*Candida albicans* at 37 °C for 120 min. Data are presented as mean ± SD (n = 3).

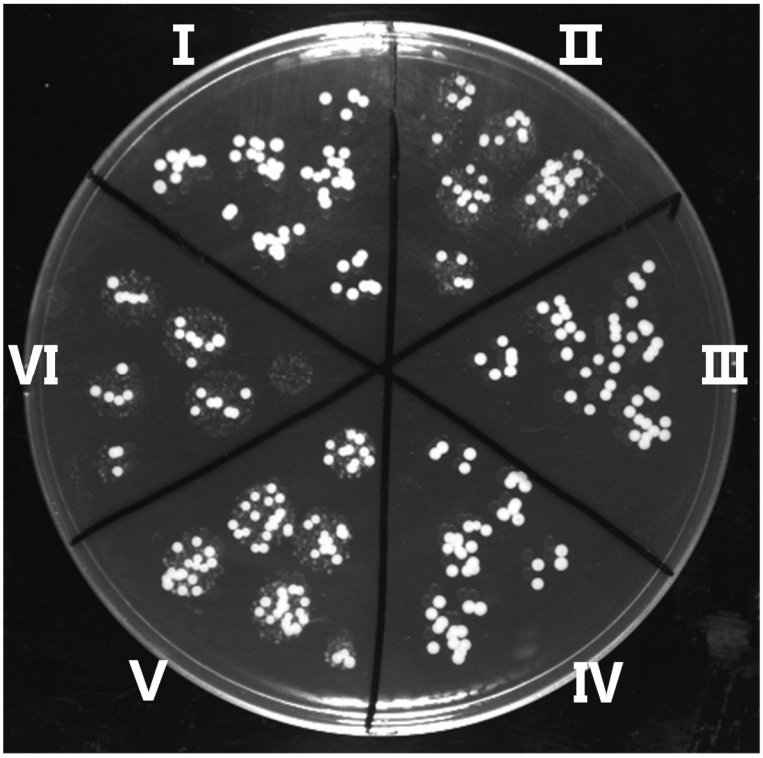

Fig. S16. Digital images of *Candida albicans* and *Lactobacillus* colonies after different treatments. I, Control; II, *Lactobacillus*-treated; III, rGO-treated; IV, rGO@FeS_2-treated; V, rGO + *Lactobacillus*-treated; VI, rGO@FeS_2 + *Lactobacillus*-treated. The co-incubation time was 24 h. *Lactobacillus* (small and transparent) and *Candida albicans* (large and milky).

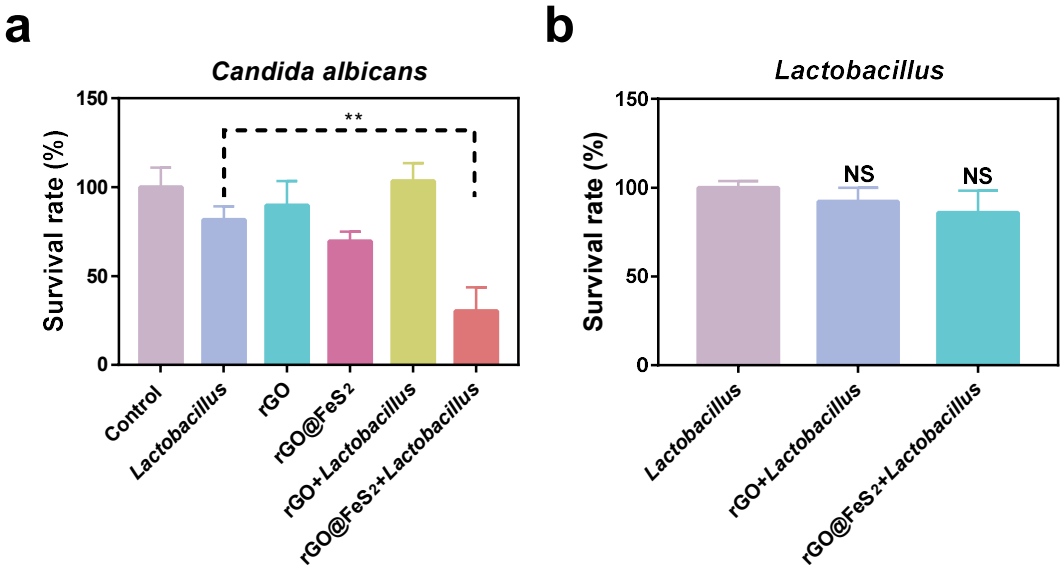

Fig. S17. *Candida albicans* cell viability (a) and *Lactobacillus* cell viability (b) in the indicated groups. Data are presented as mean ± SD (n = 3).

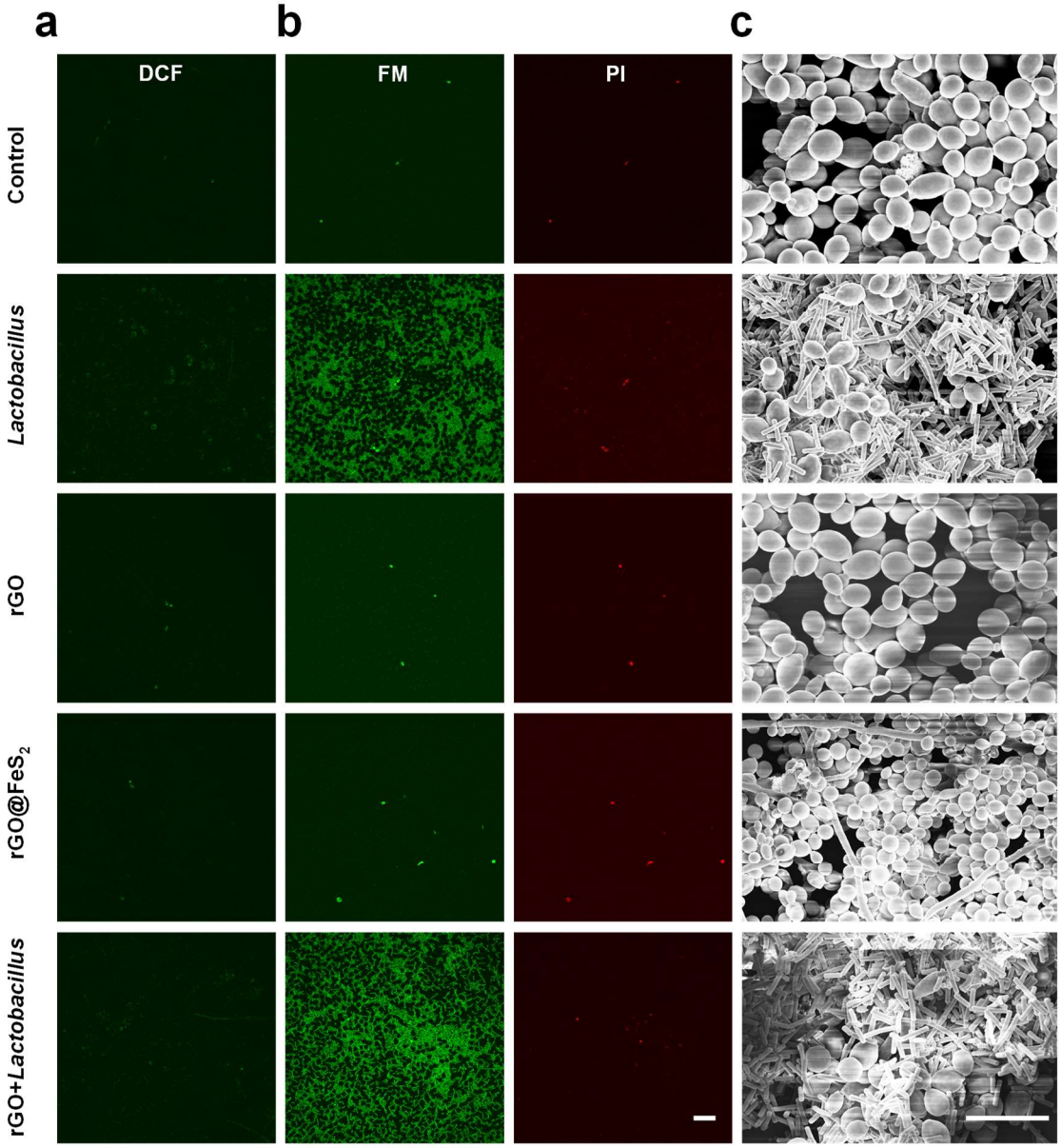

Fig. S18. ROS level (DCF) (a), cell viability (FM and PI staining) (b), and SEM images of *Candida albicans* and *Lactobacillus* (c) in different groups. The concentration of rGO was 25 μg/mL. The co-incubation time was 24 h. Scale bar: 20 μm (Left), 10 μm (Right).

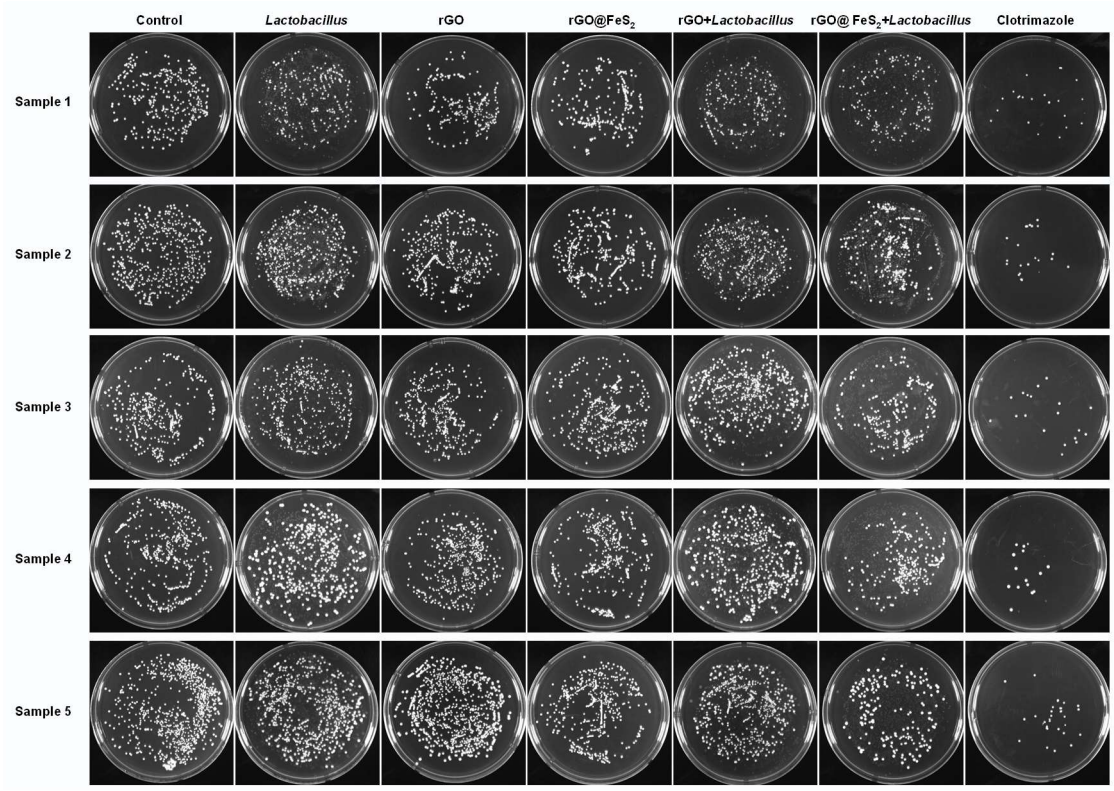

Fig. S19. Digital images of clinically isolated *Candida albicans* after indicated treatments. The co-incubation time was 24 h. *Lactobacillus* (small and transparent) and *Candida albicans* (large and milky).

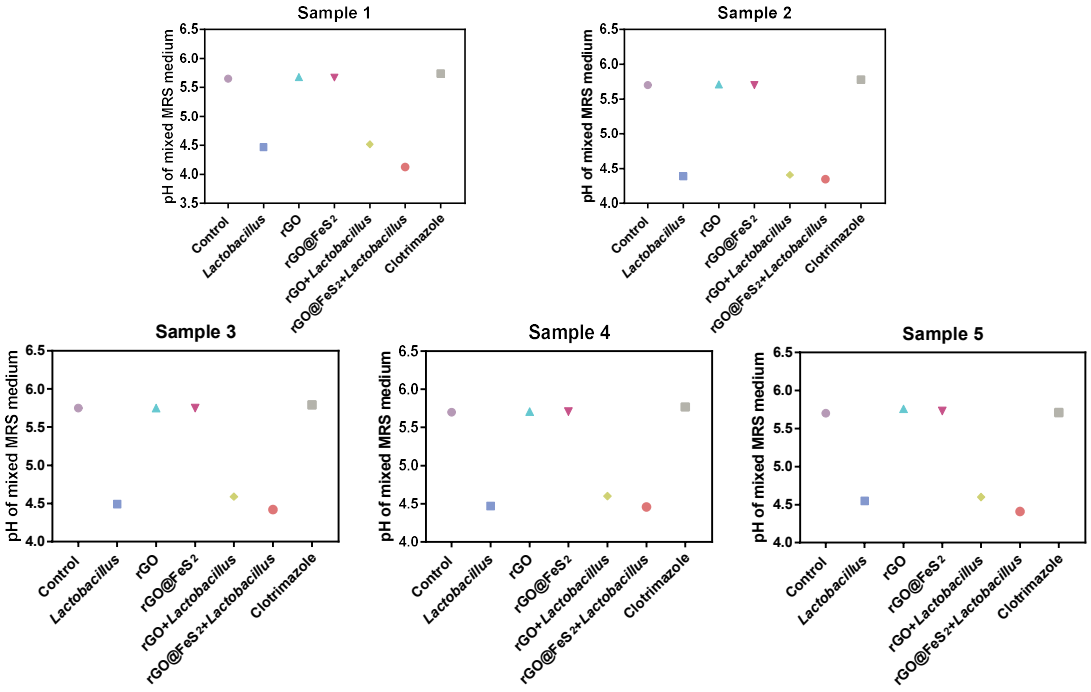

Fig. S20. pH of MRS medium incubated with clinically isolated *Candida albicans* for 24 h, followed by indicated treatments.

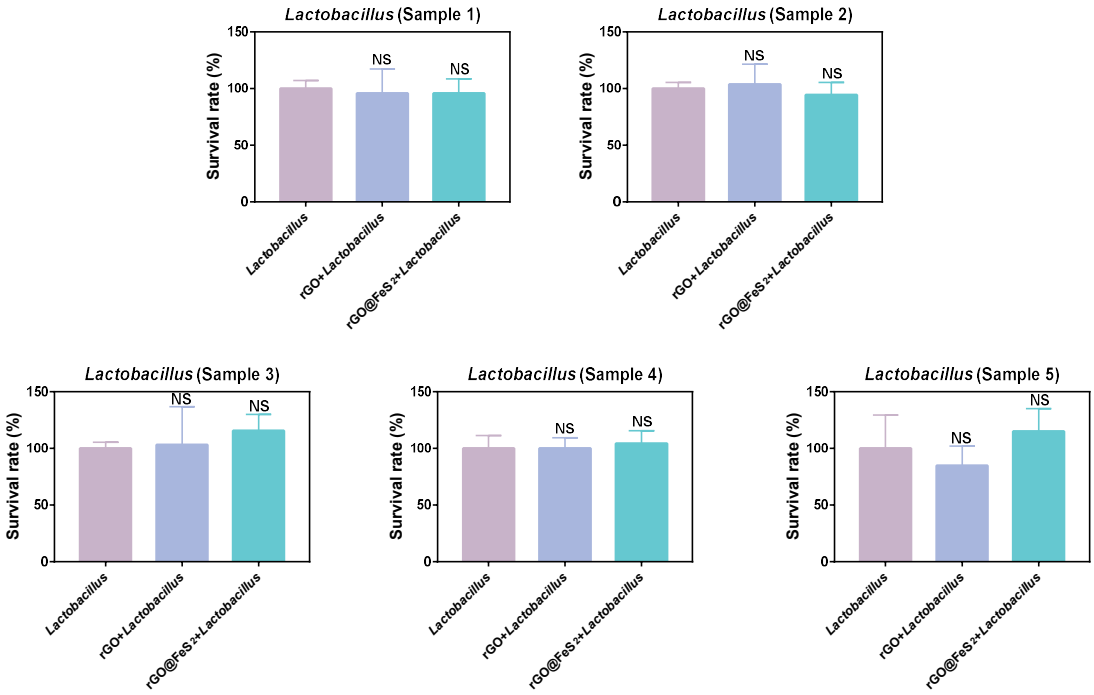

Fig. S21. *Lactobacillus* cell viability incubated with clinically isolated *Candida albicans* for 24 h, followed by indicated treatments. Data are presented as mean ± SD (n = 3).

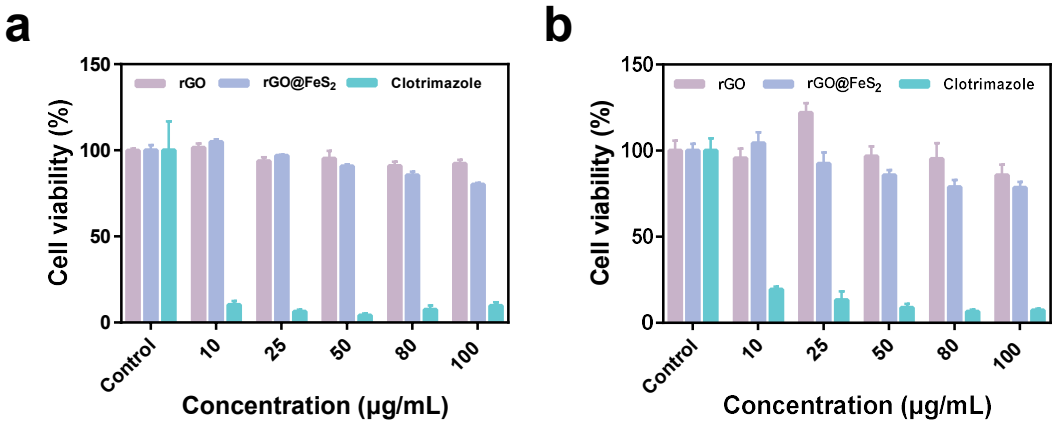

Fig. S22. Cell viability of NIH/3T3 cells (a) and L02 cells (b) after incubation for 24 h with different concentrations of rGO, rGO@FeS_2, and Clotrimazole. Data are presented as mean ± SD (n = 3).

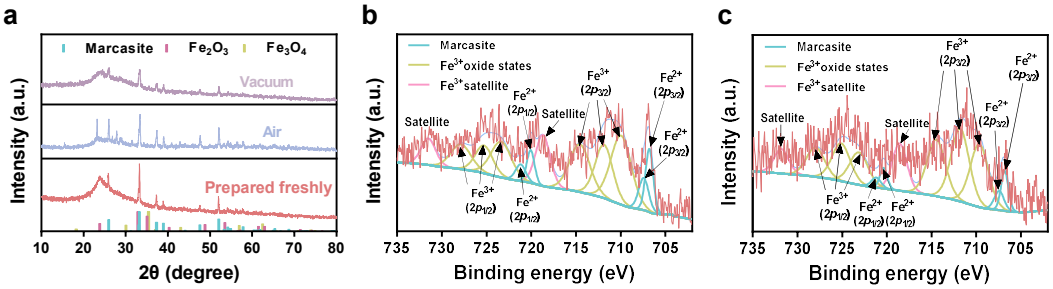

Fig. S23. XRD patterns and XPS spectra for Fe 2*p* of rGO@FeS_2 nanozymes during storage. a, XRD patterns of rGO@FeS_2 after twelve days of storage in vacuum and air. The lines at the bottom mark the reference patterns of marcasite FeS_2 (JCPDS card number 74-1051), Fe_2O_3 (JCPDS card number 88-2359), and Fe_3O_4 (JCPDS card number 72-2303). **b, c**, XPS spectra for Fe 2*p* of rGO@FeS_2 after twelve days of storage in vacuum (**b**) and air (**c**).

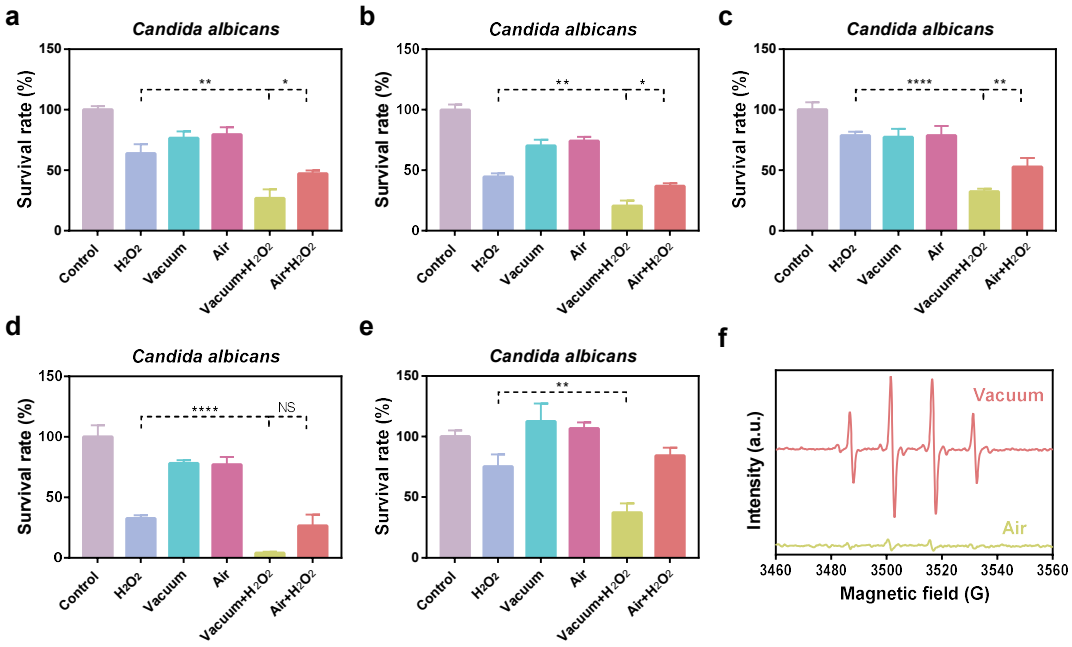

Fig. S24. Anti-*Candida albicans* and POD-like activities of oxidized rGO@FeS_2. a-e, Antifungal effects of oxidized rGO@FeS_2 with H_2O_2 on *Candida albicans* in vacuum and air for 1 (**a**), 3 (**b**), 6 (**c**), 12 (**d**), and 30 (**e**) days, respectively. **f,** EPR monitoring the generation of $^{\bullet}OH$ by rGO@FeS_2 stored in air and vacuum for 12 days in the presence of H_2O_2. Data are presented as mean ± SD (n = 3).

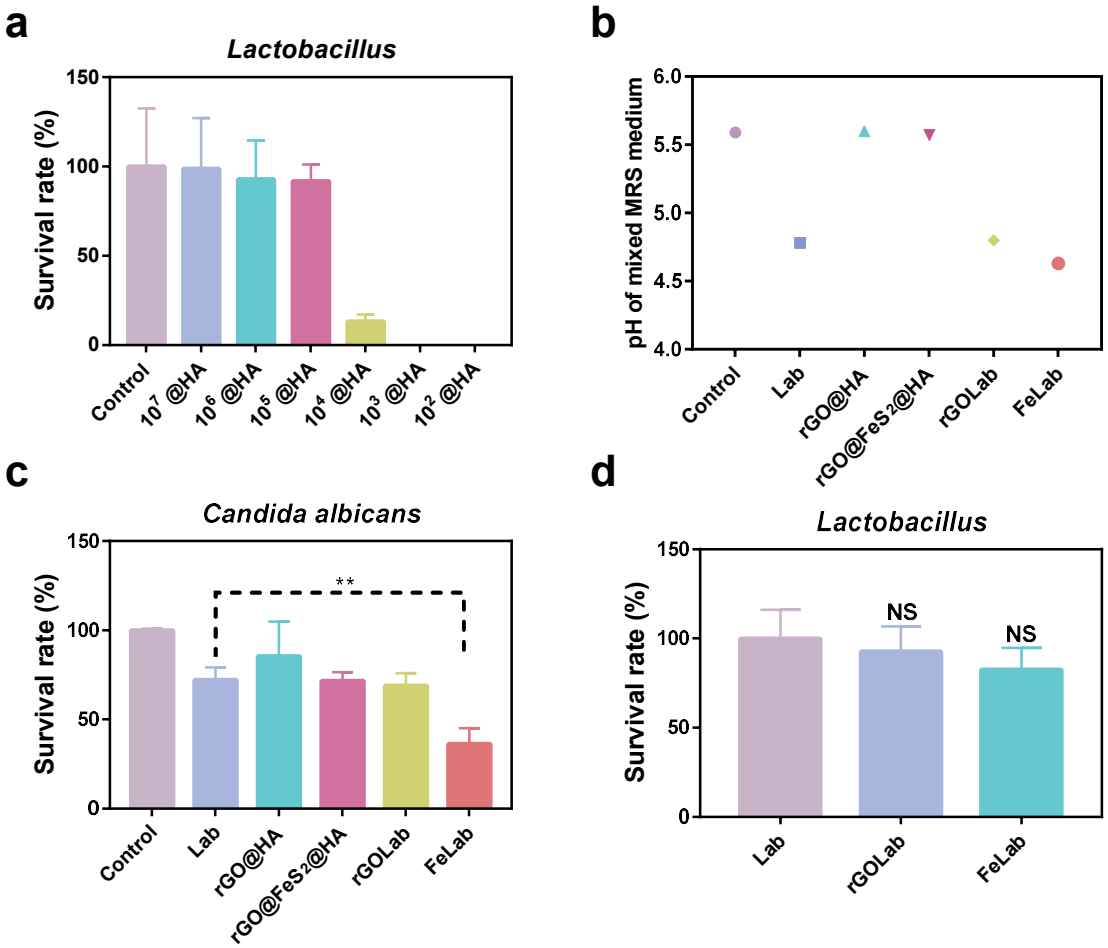

Fig. S25. Effects of FeLab on *Candida albicans* and *Lactobacillus*. a, Effects of HA coating on *Lactobacillus* cell viability. **b-d**, pH of MRS medium (**b**), *Candida albicans* cell viability (**c**) and *Lactobacillus* cell viability (**d**) after indicated treatments. Data are presented as mean ± SD (n = 3).

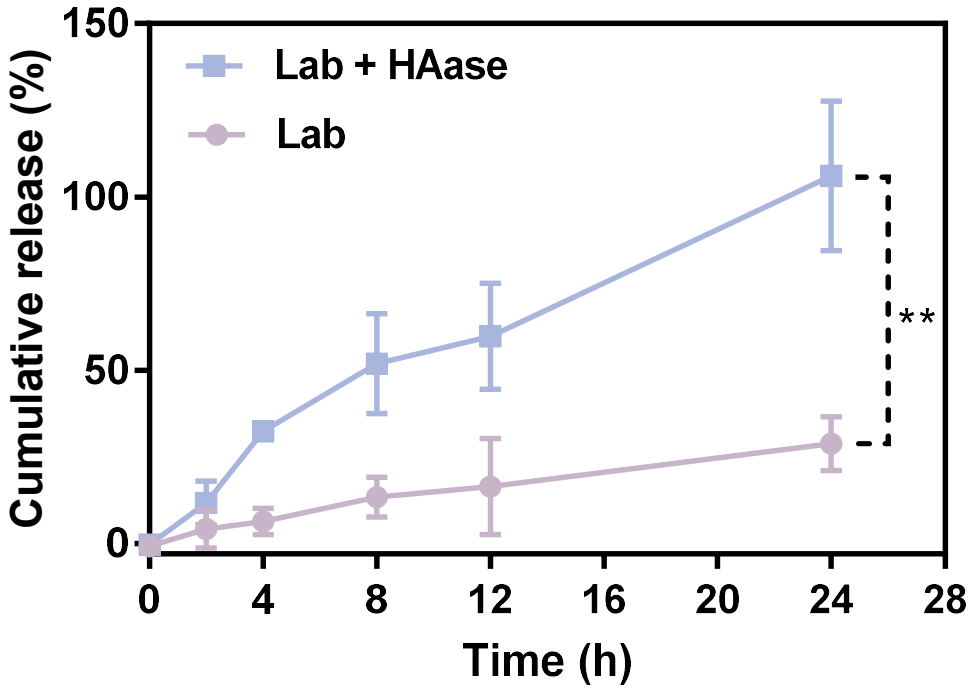

Fig. S26. Release profile of *Lactobacillus* from Lab with/without HAase solutions. The concentration of HAase was 150 U/mL. Data are presented as mean ± SD (n = 3).

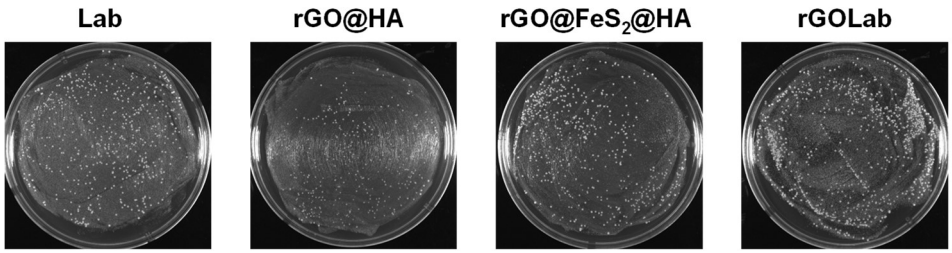

Fig. S27. Digital images of *Candida albicans* colonies in the vaginal washes after Lab, rGO@HA, rGO@FeS_2@HA, and rGOLab treatments.

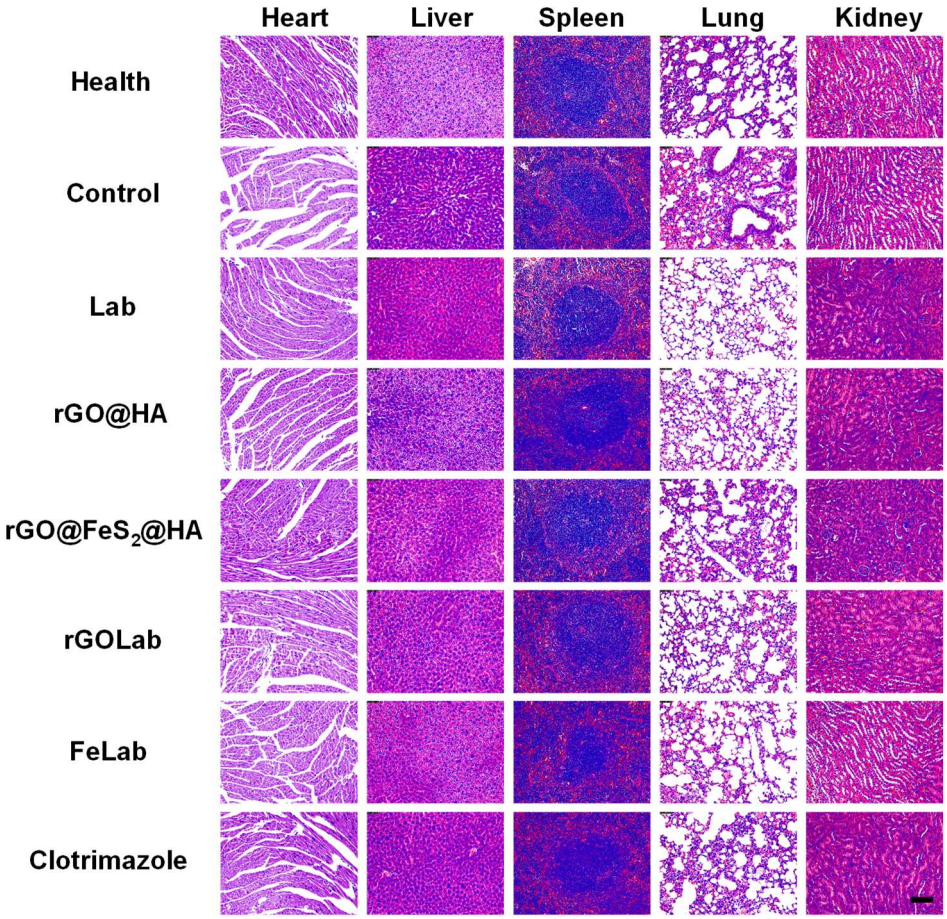

Fig. S28. HE staining images of the main organs of mice with *Candida albicans*-induced vaginitis after the indicated treatments. Scale bar: 100 μm.

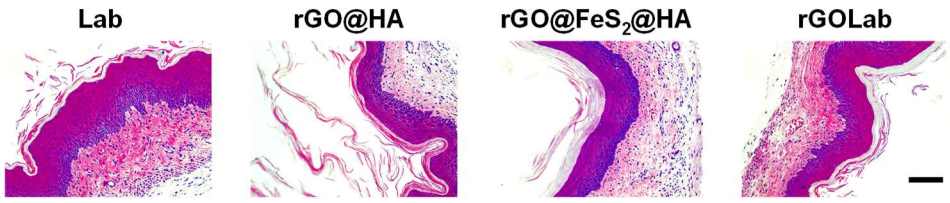

Fig. S29. HE staining images of the vaginal tissue with indicated treatments. Scale bar: 100 μm.

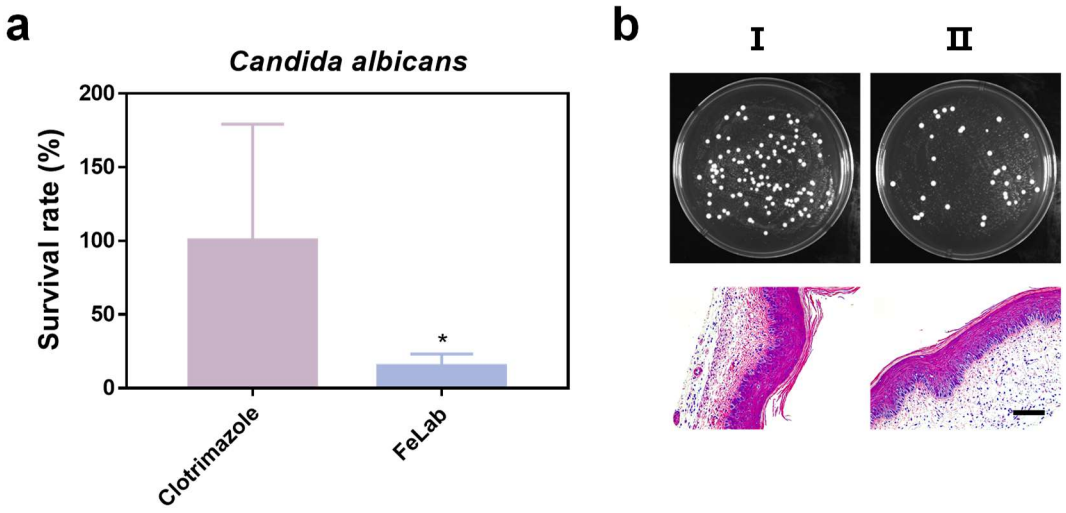

Fig. S30. Comparing recurrence of *Candida* vaginitis between FeLab and Clotrimazole. a, Cell viability of *Candida albicans* after indicated treatments. **b**, Digital images of *Candida albicans* colonies in the vaginal washes and HE staining images of the vaginal tissue of mice with recurrent *Candida* vaginitis treated with Clotrimazole (I) and FeLab (II). Scale bar: 100 μm. Data are presented as mean ± SD (n = 6).

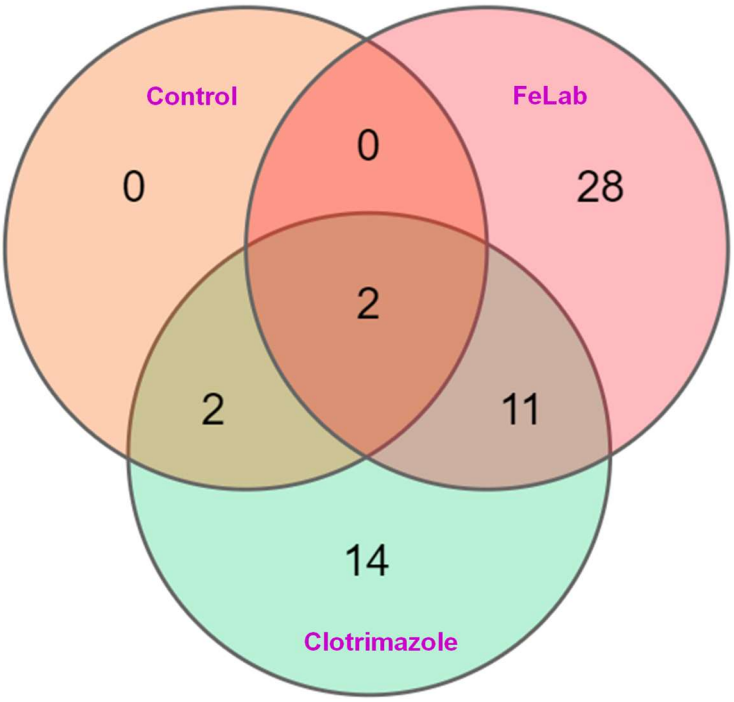

Fig. S31. Venn diagram of the shared fungi in vaginal microbiome between FeLab and Clotrimazole treatments.

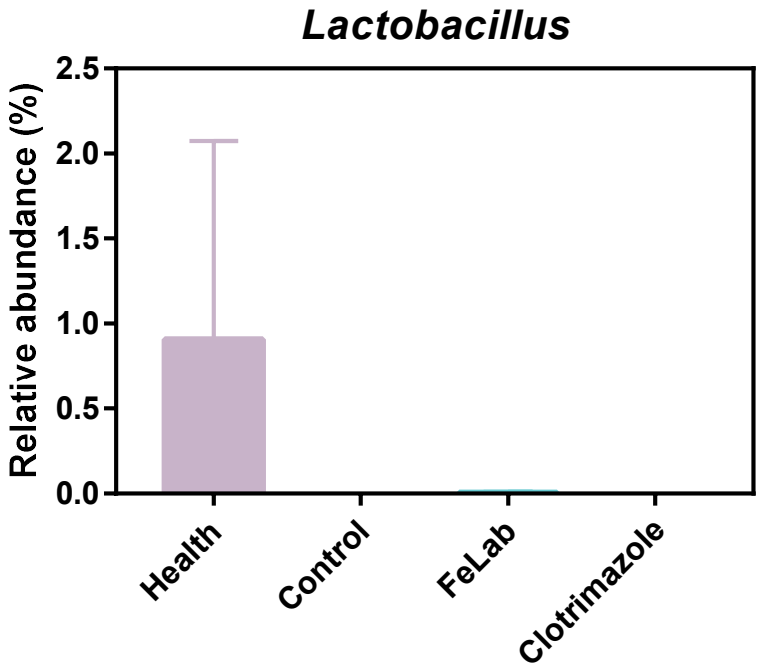

Fig. S32. Relative abundance of genus-level taxa for *Lactobacillus* between FeLab and Clotrimazole treatments. Data are presented as mean ± SD (n = 4).

Table S1. Catalytic activity and kinetic parameters for the POD-like activity of rGO@FeS_2, Pt_3Fe, Pyrite, and Fe_3O_4 nanozymes with H_2O_2 or TMB as substrate.

Nanozymes	Substrates	K_m (mM)	v_{max} (nM/s)	Mass activity (nM/s/mg)
rGO@FeS_2	H_2O_2	0.019	12.84	513.6
rGO@FeS_2	TMB	0.43	28.75	1150
Pt_3Fe	H_2O_2	0.05	4030	1.14×10^8
Pt_3Fe	TMB	0.28	5548	1.57×10^8
Pyrite	H_2O_2	0.021	5.38	283.16
Pyrite	TMB	6.42	129	6789.47
Fe_3O_4	H_2O_2	0.01	0.55	157.14
Fe_3O_4	TMB	0.66	1.71	488.57